

Equilibrium contact angle and adsorption layer properties with surfactants

Uwe Thiele,^{1,2,3,*} Jacco H. Snoeijer,⁴ Sarah Trinschek,^{1,5} and Karin John⁵

¹*Institut für Theoretische Physik, Westfälische Wilhelms-Universität Münster,
Wilhelm Klemm Str. 9, 48149 Münster, Germany*

²*Center of Nonlinear Science (CeNoS), Westfälische Wilhelms-Universität Münster, Corrensstr. 2, 48149 Münster, Germany*

³*Center for Multiscale Theory and Computation (CMTC),
Westfälische Wilhelms-Universität, Corrensstr. 40, 48149 Münster, Germany*

⁴*Physics of Fluids Group and J. M. Burgers Centre for Fluid Dynamics,
University of Twente, P.O. Box 217, 7500 AE Enschede, The Netherlands*

⁵*Université Grenoble-Alpes, CNRS, Laboratoire Interdisciplinaire de Physique, 38000 Grenoble, France*

The three-phase contact line of a droplet on a smooth surface can be characterized by the Young-Dupré equation. It relates the interfacial energies with the macroscopic contact angle θ_e . On the mesoscale, wettability is modeled by a film-height-dependent wetting energy $f(h)$. Macro- and mesoscale description are consistent if $\gamma \cos \theta_e = \gamma + f(h_a)$ where γ and h_a are the liquid-gas interface energy and the thickness of the equilibrium liquid adsorption layer, respectively.

Here, we derive a similar consistency condition for the case of a liquid covered by an insoluble surfactant. At equilibrium, the surfactant is spatially inhomogeneously distributed implying a non-trivial dependence of θ_e on surfactant concentration. We derive macroscopic and mesoscopic descriptions of a contact line at equilibrium and show that they are only consistent if a particular dependence of the wetting energy on the surfactant concentration is imposed. This is illustrated by a simple example of dilute surfactants, for which we show excellent agreement between theory and time-dependent numerical simulations.

I. INTRODUCTION

Surfactants are amphiphilic molecules or particles that adsorb at interfaces, thereby decreasing the surface tension of the interface. Their chemico-physical properties crucially alter the dynamics of thin liquid films with free surfaces, a fact that is exploited for many industrial and biomedical applications, e.g. coating, deposition or drying processes on surfaces, surfactant replacement therapy for premature infants (see [1, 2] for reviews). However, the detailed mechanism of surfactant driven flows is still an active field of research, experimentally and theoretically. In the simplest case, the spreading of surfactant laden droplets on solid surfaces, the presence of surfactants leads to deviations from the Tanner law, i.e. the spreading rate is rather $R(t) \sim t^{1/4}$ instead of $R(t) \sim t^{1/10}$ as expected for the pure liquid (see [2] for review). The basic explanation for this phenomenon is that gradients in the surface tension are associated with interfacial (Marangoni) stresses which drive the fluid flow and the convective and diffusive transport of surfactant molecules along the interface. The surfactant concentration and the interfacial tension are related by an equation of state.

Besides the modified Tanner law, the interplay between surfactant dynamics and free surface thin film flows leads to a variety of intriguing phenomena, such as surfactant induced fingering of spreading droplets [2–7], super-spreading of aqueous droplets on hydrophobic surfaces [8, 9], or autophobing of aqueous drops on hydrophilic

substrates [10–12]. In addition to creating Marangoni stresses at the free interface, several other properties of surfactants enrich the spectrum of dynamical behaviors observed. Bulk solubility, their propensity to form micelles or lamellar structures at high concentrations, the surfactant mobility on the solid surface and their ability to spread through the three-phase contact region are all key parameters to influence the flow properties. But the presence of surfactants does not only affect the flow dynamics. Also in the static situation of a surfactant-covered droplet on a substrate in equilibrium, the spatially inhomogeneous distribution of surfactant will cause a non-trivial dependence of the contact angle on the surfactant concentration.

The governing equations that describe film flows and surfactant dynamics at low surfactant concentrations and in situations where the influence of wettability is negligible are well established (see [13, 14] for review). Typically, the dynamics of the liquid with a free surface is described using an evolution equation for the film height (derived from the lubrication approximation of a viscous Stokes flow with no-slip boundary condition at the substrate) coupled to an evolution equation of the surfactant concentration. The equations usually include capillarity (with a constant surface tension, though) and Marangoni stresses via an equation of state for the surfactant. Some models include wettability via a disjoining pressure [11, 15, 16]. However, often specific model features, e.g. nonlinear equations of state are included at the level of the dynamic equations in an ad hoc fashion, neglecting thereby the fact, that the passive surfactant-thin film system has to respect symmetries imposed by the laws of thermodynamics (see [13] for review).

The recent formulation of the dynamic equations in

* u.thiele@uni-muenster.de

terms of a thermodynamically consistent gradient dynamics [13, 14] sheds some light on a more rigorous approach to model surfactant driven thin film flows using an energy functional. Following the approach from Refs. [13, 14], features like nonlinear equations of state for the surfactant and concentration-dependent wettability can be included in a consistent manner into a mesoscopic description. However, what still needs to be established is the consistency of the mesoscopic approach with macroscopic parameters, i.e. the equilibrium contact angle of a droplet in the presence of surfactants. This relation has been derived by Sharma [17] for droplets of pure liquids on a solid substrate, by relating the mesoscopic parameters of the wetting energy to the macroscopic Young-Dupré equation and is e.g. also discussed in [18] for different wetting scenarios.

Here we establish this mesoscopic-macroscopic link for the extended system: a droplet of a pure liquid in contact with a solid substrate covered by a liquid adsorption layer in the presence of insoluble surfactants. Our approach is based on a mesoscopic energy functional depending on the film height and the surfactant coverage profiles. We reveal the selection of the contact angle θ_e in the presence of surfactants. This involves a nontrivial coupling with the equilibration of surfactant concentrations, respectively on the drop and on the liquid adsorption layer. These considerations are relevant for cases involving bare substrates or ultra thin films, where apolar and/or polar forces between interfaces become non-negligible and where the dynamics is governed by the contact line. For example, it has been proposed that the onset of Marangoni flows for surfactant driven spreading and fingering of droplets on hydrophilic surfaces depends on the ability of the surfactant to diffuse in front of the droplet to establish a gradient, which then drives the flow [6, 7]. Similarly, autophobing is associated with a transfer of surfactant onto the substrate to render it less hydrophilic [10, 11], leading to dewetting and film rupture. Although surfactant induced flows are dynamic phenomena out of equilibrium, the underlying theoretical framework of linear flux-force relations has to be consistent with the equilibrium conditions at the meso- and macroscale.

The paper is structured as follows: First in section II, we will revise how to derive the macroscopic and mesoscopic equilibrium descriptions for a surfactant-free droplet of a pure liquid on a solid substrate. This parallel approach establishes the link between the macroscopic variables (surface tensions) and the additional mesoscopic variables (wetting energy) via the Young-Dupré law. While this section gives identical results as Ref. [17], it is nevertheless a pedagogical introduction to the more involved calculations in the presence of surfactants, which constitutes section III of the paper. We rely here strictly on the existence of a (generalized) Hamiltonian, which includes capillarity and a wetting energy, both dependent on the surfactant concentration. No other assumptions about the underlying hydrodynamics of the problem are

made. We show the conditions for consistency between the macroscopic and mesoscopic approach in terms of the equilibrium contact angle and the equilibrium distribution of surfactants. In section IV, we illustrate our calculations by explicitly choosing a functional form for the Hamiltonian, consistent with a linear equation of state for the surfactant and we propose a simple modification of the disjoining pressure which yields consistency with the Young-Dupré law in the presence of surfactants.

II. A DROP OF SIMPLE LIQUID (NO SURFACTANTS)

A. Macroscopic consideration

We start by reviewing the derivation of the Laplace pressure and the Young-Dupré law from a free energy approach that we will later expand by incorporating surfactants. Let us consider a 2D liquid drop of finite volume, i.e., a cross section of a transversally invariant liquid ridge, that has contact lines at $x = \pm R$ (see sketch Fig. 1 (a)). The liquid-gas, solid-liquid and solid-gas free energy per area here directly correspond to the interface tensions and are denoted by Υ , Υ_{sl} and Υ_{sg} , respectively. Using the drop's reflection symmetry the (half) free energy is

$$\mathcal{F} = \int_0^R dx [\Upsilon\xi + \Upsilon_{sl} - Ph] + \int_R^\infty dx \Upsilon_{sg} + \lambda_h h(R). \quad (1)$$

where the metric factor is

$$\xi = (1 + (\partial_x h)^2)^{1/2} \quad (2)$$

and ∂_x denotes the derivative w.r.t. x . For small interface slopes one can make the small-gradient or long-wave approximation

$$\xi \approx 1 + (\partial_x h)^2/2 \quad (3)$$

often used in gradient dynamics models on the interface Hamiltonian (aka thin-film or lubrication models) [19–21]. The liquid volume $V = \int dx h$ is controlled via the Lagrange multiplier P .

We independently vary the profile $h(x)$ and the position of the contact line R . The two are coupled due to $h(R) = 0$, which is imposed through the Lagrange multiplier λ_h . Varying $h(x)$ implies

$$\delta\mathcal{F} = \left[\Upsilon \frac{\partial_x h}{\xi} + \lambda_h \right] \delta h(R) - \int_0^R dx \delta h(x) \left[\Upsilon \frac{\partial_{xx} h}{\xi^3} + P \right] \quad (4)$$

which gives

$$\lambda_h = -\Upsilon \frac{\partial_x h}{\xi}, \quad \text{for } x = R, \quad (5)$$

$$P = -\Upsilon \kappa, \quad \text{for } x \in [0, R], \quad (6)$$

where we introduced the curvature

$$\kappa = \frac{\partial_{xx} h}{\xi^3}. \quad (7)$$

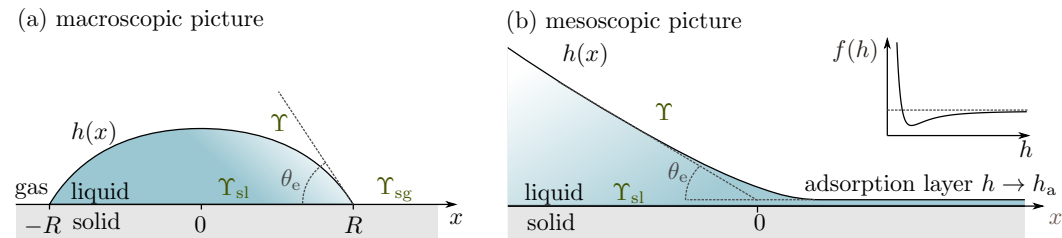


FIG. 1. Liquid drop at a solid-gas interface. (a) In the macroscopic picture, the equilibrium contact angle θ_e is determined by the interfacial tensions Υ , Υ_{sl} and Υ_{sg} , characterizing the liquid-gas, solid-liquid and solid-gas interface, respectively. (b) In the mesoscopic picture, the substrate is covered by an equilibrium adsorption layer of height h_a which corresponds to the minimum of the wetting energy $f(h)$.

The variation of R evaluated at $x = R$ gives

$$\delta\mathcal{F} = [\Upsilon\xi + \Upsilon_{sl} - \Upsilon_{sg} - Ph + \lambda_h(\partial_x h)]\delta R \quad (8)$$

which together with the constraint $h(R) = 0$ and λ_h [Eq. (5)] results in the Young-Dupr e law

$$\Upsilon \cos \theta_e = \Upsilon_{sg} - \Upsilon_{sl}, \quad (9)$$

where we employed

$$1/\xi = (1 + (\partial_x h(R))^2)^{-1/2} = \cos \theta_e. \quad (10)$$

Note that a similar approach is also presented in [22] and in [23], where a transversality condition at the boundary is used instead of a Lagrange multiplier that fixes $h(R) = 0$. Next, we remind the reader how to obtain the same law from considerations on the mesoscale.

B. Mesoscopic consideration

Now we start from an interface Hamiltonian derived from microscopic considerations, asymptotically or numerically (see e.g., Refs. [24–27])

$$\mathcal{F} = \int_0^\infty dx [\Upsilon\xi + \Upsilon_{sl} + f(h) - Ph] \quad (11)$$

with the same metric factor defined in (2). As in (1) we consider only the half energy of a reflection symmetric droplet. Here $f(h)$ is the wetting potential [24, 25] as depicted in Fig. 1 (b). For partially wetting liquids $f(h)$ normally has a minimum at some $h = h_a$ corresponding to the height of an equilibrium adsorption layer (in hydrodynamics often referred to as “precursor film”) and approaches zero as $h \rightarrow \infty$. Mathematically, \mathcal{F} is a Lyapunov functional, thermodynamically it may be seen as a grand potential, and in a classical mechanical equivalent it would be an action (i.e., the integral over the Lagrangian, with position x and film height h taking the roles of time and position in classical point mechanics).

Now we vary \mathcal{F} w.r.t. $h(x)$ and obtain

$$\delta\mathcal{F} = \int_0^\infty dx \delta h(x) [-\Upsilon\kappa + \partial_h f - P] \quad (12)$$

where we used $[\Upsilon \frac{\partial_x h}{\xi} \delta h(x)]_0^\infty = 0$. Based on (12), the free surface profile is given by the Euler-Lagrange equation

$$0 = -\Upsilon\kappa + \partial_h f - P. \quad (13)$$

Multiplying by $\partial_x h$ and integrating w.r.t. x gives the ‘first integral’¹

$$\begin{aligned} E &= -\Upsilon \int \frac{\partial_x h}{\xi^3} \partial_{xx} h dx + f(h) - Ph + \Upsilon_{sl} \\ &= \frac{\Upsilon}{\xi} + f(h) - Ph + \Upsilon_{sl}, \end{aligned} \quad (14)$$

where E is a constant that is independent of x . This first integral can be interpreted as an energy density or as the horizontal force acting on a cross-section of the film. The fact that E is constant reflects the horizontal force balance.

Now we consider the wedge geometry in Fig. 1(b) and determine the thickness h_a of the coexisting adsorption layer on the right and the angle θ_e formed by the wedge on the left. To do so, we first consider Eqs. (13) and (14) in the wedge region far away from the adsorption layer, i.e., where the film height is sufficiently large that $f, \partial_h f \rightarrow 0$ and $hP \rightarrow 0$. Note, that the mesoscopic wedge region with $\partial_x h \approx \text{const}$ is distinct from the region of the macroscopic droplet governed by the Laplace law $P = -\Upsilon\kappa$ (For a more extensive argument see Ref. [17]). This gives

$$P = 0 \quad (15)$$

$$E = \frac{\Upsilon}{\xi_w} + \Upsilon_{sl} \quad (16)$$

in the wedge. Second, we consider the adsorption layer far away from the wedge. There, Eqs. (13) and (14) result in

$$P = \partial_h f|_{h_a} \quad (17)$$

$$E = \Upsilon + f(h_a) - h_a P + \Upsilon_{sl}. \quad (18)$$

¹ Note, that if the integrand of (11) is seen as Lagrangian L , the generalized coordinate and corresponding momentum are $q = h$ and $p = \partial L / \partial(\partial_x h) = \Upsilon(\partial_x h) / \xi$, respectively. Then the first integral E corresponds to the negative of the Hamiltonian $H = p \partial_x q - L$.

Equilibrium states are characterized by a pressure P and a first integral E that are constant across the system. Therefore, the adsorption layer height h_a and the contact angle θ_e are given by

$$P = \partial_h f|_{h_a} = 0 \quad \text{and} \quad (19)$$

$$\frac{\Upsilon}{\xi_w} = \Upsilon \cos \theta_e = \Upsilon + f(h_a) \quad (20)$$

respectively.

C. Consistency of mesoscopic and macroscopic approach

Comparing Eq. (20) with the macroscopic Young-Dupré law (9) in section II A yields the expected relation

$$f(h_a) = \Upsilon_{\text{sg}} - \Upsilon_{\text{sl}} - \Upsilon = S \quad (21)$$

as condition for the consistency of mesoscopic and macroscopic description. S denotes the spreading coefficient. For small contact angles $\theta_e \ll 1$, Eq. (20) reads $f(h_a) = -\Upsilon \theta_e^2/2$.

We can now reinterpret the free energy in (11). The solid substrate with adsorption layer corresponds to the “dry” region in the macroscopic free energy (1). For consistency at the energy level, the mesoscopic energy density should approach Υ_{sg} in the adsorption layer at $P = 0$ and consequently $f(h_a) = \Upsilon_{\text{sg}} - \Upsilon_{\text{sl}} - \Upsilon$, which leads also to relation (21)².

As an aside, we note that the here presented calculation is not exactly equivalent to the determination of a binodal for a binary mixture where coexistence of two homogeneous phases is characterized by equal chemical potential and equal local grand potential. Here, the coexistence of a homogeneous phase (adsorption layer) and an inhomogeneous phase (wedge) is characterized by equal pressure P (corresponding to the chemical potential in the case of a binary mixture) and equal Hamiltonian E (which differs from the local grand potential, i.e., the integrand in (11) by a factor $1/\xi^2$ in the liquid-gas interface term).

² The solid substrate with adsorption layer corresponds to the “moist case” in [28], where the energy density should approach Υ_{sg} (strictly speaking $\Upsilon_{\text{sg}}^{\text{moist}}$) and consequently $f(h_a) = \Upsilon_{\text{sg}}^{\text{moist}} - \Upsilon_{\text{sl}} - \Upsilon$ as for a flat equilibrium adsorption layer at $P = 0$. This implies that the “moist” spreading coefficient is $S^{\text{moist}} = f(h_a)$ which is well defined as long as $f(h)$ has a minimum. Note that for $h \rightarrow 0$, in many approximations the wetting energy $f(h)$ shows an unphysical divergence. This may be avoided by employing a cut-off (see e.g., [22, 28] or by determining $f(h)$ from proper microscopic models [26, 27, 29, 30]). In the latter case one finds a finite $f(0) = \Upsilon_{\text{sg}}^{\text{dry}} - \Upsilon_{\text{sl}} - \Upsilon = S^{\text{dry}}$ well defined even for $f(h)$ without minimum.

III. A LIQUID DROP COVERED BY INSOLUBLE SURFACTANTS

A. Macroscopic consideration

We now consider insoluble surfactants, which exhibit a number density Γ (per unit area) on the free liquid-gas interface $h(x)$ (see Fig. 2(a)). There may also be surfactant at the solid-gas interface. The total amount of surfactant, $N = \int ds \Gamma = \int dx \xi \Gamma$, is conserved, which is imposed by a Lagrange multiplier λ_Γ . The liquid volume $V = \int dx h$ and the condition $h(R) = 0$ for a contact line at R are ensured via Lagrange multipliers P and λ_h , respectively (as in section II A). The surface free energies of the liquid-gas and solid-gas interfaces are characterized by the functions $g(\Gamma)$ and $g_{\text{sg}}(\Gamma)$ respectively. The solid-liquid interface is assumed to be free of surfactant.

As for the case of pure liquid in section II A, we first consider a macroscopic formulation in which the interaction of the liquid-gas interface (and surfactants) with the solid near the three-phase contact line is not made explicit – this is done in the mesoscopic model presented in section III B below.

The energy now to be minimized corresponds to a grand potential and reads

$$\begin{aligned} \mathcal{F}[h, \Gamma] = & \int_0^R dx [\xi g(\Gamma) + \Upsilon_{\text{sl}} - Ph] + \int_R^\infty dx g_{\text{sg}}(\Gamma) \\ & - \lambda_\Gamma \left(\int_0^R dx \xi \Gamma + \int_R^\infty dx \Gamma \right) + \lambda_h h(R). \end{aligned} \quad (22)$$

Varying the field $\Gamma(x)$ gives

$$\delta F = \int_0^R dx \xi (\partial_\Gamma g - \lambda_\Gamma) \delta \Gamma + \int_R^\infty dx (\partial_\Gamma g_{\text{sg}} - \lambda_\Gamma) \delta \Gamma \quad (23)$$

resulting in

$$\begin{aligned} \lambda_\Gamma &= \partial_\Gamma g \quad \text{for } x \in [0, R] \\ \text{and } \lambda_\Gamma &= \partial_\Gamma g_{\text{sg}} \quad \text{for } x \in [R, \infty]. \end{aligned} \quad (24)$$

Since, in general, $\partial_\Gamma g$ is a function of Γ and λ_Γ is a constant, Eq. (24) implies that the surfactant is homogeneously distributed in each region, i.e.,

$$\partial_x \Gamma = 0. \quad (25)$$

We introduce the equilibrium concentrations $\Gamma(x) = \Gamma_d$ on the droplet and $\Gamma(x) = \Gamma_a$ on the substrate. For the equilibrium distribution of surfactants with constant chemical potential λ_Γ , Eq. (24) reduces to

$$\partial_\Gamma g|_{\Gamma_d} = \partial_\Gamma g_{\text{sg}}|_{\Gamma_a}. \quad (26)$$

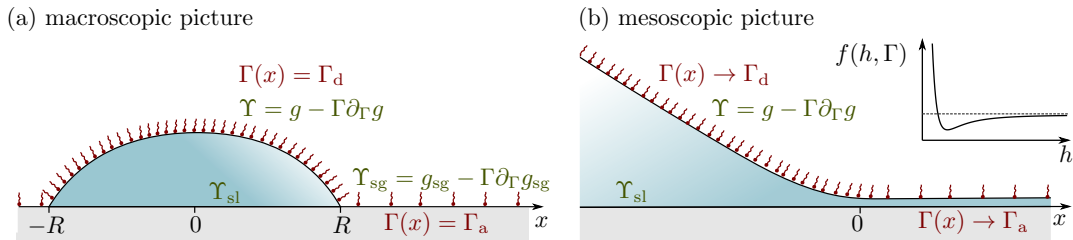


FIG. 2. Liquid drop covered by insoluble surfactant at a solid-gas interface. (a) In the macroscopic approach, the equilibrium contact angle is determined by the solid-liquid interfacial tension Υ_{sl} and the interfacial tensions Υ and Υ_{sg} , which describe the liquid-gas and the the solid-gas interfacial tension and which depend on the respective surfactant concentrations Γ_d and Γ_a on the droplet and the adsorption layer. (b) In the mesoscopic picture, the substrate is covered by an equilibrium adsorption layer and the contact angle is determined by the liquid-gas interfacial tension Υ which depends on the surfactant concentration, the solid-liquid interfacial tension Υ_{sl} and the minimum of the wetting energy $f(h_a)$.

Varying the field $h(x)$ gives

$$\begin{aligned} \delta\mathcal{F} &= \int_0^R dx \left[-P - \frac{\partial_{xx}h}{\xi^3} (g - \lambda_\Gamma \Gamma) \right] \delta h(x) \\ &\quad + \left[\left(\frac{\partial_x h}{\xi} (g - \lambda_\Gamma \Gamma) \right) \delta h \right]_0^R + \lambda_h \delta h(R) \\ &= \int_0^R dx [-P - \kappa \Upsilon] \delta h(x) + \left[\frac{\partial_x h}{\xi} \Upsilon + \lambda_h \right] \delta h(R) \end{aligned} \quad (27)$$

where we employed Eq. (24) and introduced the surfactant-dependent liquid-gas interface tension (aka local grand potential, aka mechanical tension in the interface or surface stress)

$$\Upsilon = g - \Gamma \partial_\Gamma g. \quad (28)$$

Note that indeed for insoluble surfactants a Wilhelmy plate in a Langmuir trough measures Υ and not g as the area is changed at fixed amount of surfactant, i.e., Γ changes with the area. At the left boundary at $x = 0$, the reflection symmetry of the droplet enforces $\partial_x h = 0$. Eq. (27) implies that the Laplace pressure and λ_h become

$$P = -\Upsilon \kappa, \quad \text{for } x \in [0, R] \quad (29)$$

$$\lambda_h = -\Upsilon \frac{\partial_x h}{\xi}, \quad \text{at } x = R. \quad (30)$$

Finally, variation of R evaluated at $x = R$ gives:

$$\begin{aligned} \delta\mathcal{F} &= [\xi g(\Gamma) + \Upsilon_{sl} - Ph - g_{sg}(\Gamma_a) - \lambda_\Gamma \xi \Gamma_d \\ &\quad - \lambda_\Gamma \Gamma_a + \lambda_h \partial_x h(R)] \delta R \end{aligned} \quad (31)$$

Using the constraint $h(R) = 0$, as well as the obtained values for λ_Γ and λ_h , this gives the boundary condition (using $1/\xi = \cos \theta_e$):

$$0 = \Upsilon_{sl} - \Upsilon_{sg}(\Gamma_a) + \Upsilon(\Gamma_d) \cos \theta_e \quad (32)$$

$$\text{with } \Upsilon(\Gamma_d) = g(\Gamma_d) - \Gamma_d \partial_\Gamma g|_{\Gamma_d}, \quad (33)$$

$$\text{and } \Upsilon_{sg}(\Gamma_a) = g_{sg}(\Gamma_a) - \Gamma_a \partial_\Gamma g_{sg}|_{\Gamma_a}, \quad (34)$$

i.e., we have again found the Young-Dupré law that relates interfacial tensions and equilibrium contact angle. However, the interface tensions Υ_i are not based on the local free energies g and g_{sg} (which would enter at fixed concentration Γ), but on the local grand potentials $g - \Gamma \partial_\Gamma g$ and $g_{sg} - \Gamma \partial_\Gamma g_{sg}$ (valid at constant total amount of surfactant).

Importantly, the values of Υ and Υ_{sg} are not fixed a priori, but have to be determined self-consistently from the equilibration of surfactant concentration, as given by (26). As such, the observed contact angle involves a subtle coupling between mechanics and distribution of surfactants.

B. Mesoscopic consideration

In analogy to section IIB where we developed mesoscopic considerations in the case without surfactant, next we discuss how to describe the case of insoluble surfactants on the mesoscale. Again we focus on equilibrium situations involving a contact line (Fig. 2(b)). Now it needs to be discussed how the dependency of the wetting potential on surfactant concentration has to be related to the respective dependencies of the involved surface energies to ensure consistency of mesoscopic and macroscopic descriptions.

A general discussion of a gradient dynamics description for the dynamics of liquid layers or drops covered by insoluble or soluble surfactants can be found in [13] and [14], respectively. There, various thermodynamically consistent extensions of thin film hydrodynamics without surfactants towards situations with surfactants are discussed and contrasted to literature approaches. Such extensions are, for instance, surfactant-dependent interface energies and wetting potentials that affect not only hydrodynamic flows but also diffusive fluxes. However, the intrinsic relations between wetting energy f and interface energies g were not discussed.

To begin with, we consider a general wetting energy $f(h, \Gamma)$ and interface energies $g(\Gamma)$. The resulting grand

potential is

$$F[h, \Gamma] = \int_0^\infty [\Upsilon_{sl} + f(h, \Gamma) + g(\Gamma)\xi - Ph - \lambda_\Gamma \Gamma \xi] dx \quad (35)$$

with ξ being again the metric factor (2). P and λ_Γ are the Lagrange multipliers for the conservation of the amounts of liquid and surfactant, respectively. Note that we treat the solid-liquid interface energy Υ_{sl} as constant.

Varying $h(x)$ and $\Gamma(x)$, we obtain from (35) the Euler-Lagrange equations

$$P = \partial_h f - \partial_x [(g - \lambda_\Gamma \Gamma) \frac{\partial_x h}{\xi}] \quad (36)$$

$$\text{and } \lambda_\Gamma = \frac{1}{\xi} \partial_\Gamma f + \partial_\Gamma g, \quad (37)$$

respectively, i.e., the pressure P and chemical potential λ_Γ are constant across the system.

We use the mechanical approach of footnote 1 and introduce the generalized positions $q_1 = h$ and $q_2 = \Gamma$ and obtain from the local grand potential (integrand in (35), i.e., the 'Lagrangian'), the generalized momenta $p_1 = (g - \lambda_\Gamma \Gamma)(\partial_x h)/\xi$ and $p_2 = 0$, respectively. In consequence, the first integral E is

$$E = \Upsilon_{sl} + f + \frac{g - \Gamma \lambda_\Gamma}{\xi} - hP \quad (38)$$

i.e., Eq. (14) with Υ replaced by $g(\Gamma) - \Gamma \lambda_\Gamma$. All equilibrium states are characterized by P , λ_Γ and E that are constant across the system. This allows us to investigate the coexistence of states.

As in section II B, we consider the equilibrium between a wedge region with constant slope $\tan \theta_e$ and an adsorption layer of thickness h_a (Fig. 2(b)). As the wetting potential $f(h, \Gamma)$ depends on film height and surfactant concentration, one does not only need to determine the coexisting wedge slope and adsorption layer height as in section II B but also the coexisting surfactant concentrations on the wedge, Γ_w , and on the adsorption layer, Γ_a . The considered wedge is far away from the adsorption layer ($h \gg h_a$, $f \rightarrow 0$, $|\partial_x h| \rightarrow \tan \theta_e$, $\Gamma \rightarrow \Gamma_w$) and the adsorption layer is far away from the wedge ($h \rightarrow h_a$, $\partial_x h \rightarrow 0$, $\Gamma \rightarrow \Gamma_a$), i.e., both are sufficiently far away from the contact line region. By comparing P , λ_Γ and E from Eqs. (36), (37) and (38) in wedge and adsorption layer (in analogy to the calculation in section II B), one finds

$$0 = \partial_h f|_{(h_a, \Gamma_a)}, \quad (39)$$

$$\partial_\Gamma g|_{\Gamma_w} = \partial_\Gamma f|_{(h_a, \Gamma_a)} + \partial_\Gamma g|_{\Gamma_a}, \quad (40)$$

$$\Upsilon(\Gamma_w) \cos \theta_e = f(h_a, \Gamma_a) - \Gamma_a \partial_\Gamma f|_{(h_a, \Gamma_a)} + \Upsilon(\Gamma_a), \quad (41)$$

respectively. To obtain (41) we have already used (39) and (40) as well as $\xi_w = 1/\cos \theta_e$ and (28). Without surfactant we recover Eq. (20) of section II B as $g(0)$ is Υ of Sec. II.

The obtained Eqs. (39) to (41) allow one to determine the 'binodals' for the wedge-adsorption layer coexistence. In practice, one may choose any of the four

quantities $\theta_e, \Gamma_w, h_a, \Gamma_a$ as control parameter and determine the other three from the three relations (39)-(41). It is convenient to pick Γ_a as control parameter and first use Eq. (39) to determine h_a , then employ Eq. (40) to obtain Γ_w and, finally, Eq. (41) to get the equilibrium contact angle θ_e . To obtain specific results, the wetting energy $f(h, \Gamma)$ and free energies of the liquid-gas interface $g(\Gamma)$ and the solid-gas interface $g_{sg}(\Gamma)$ have to be specified. A simple but illustrative example is discussed in section IV.

C. Consistency of mesoscopic and macroscopic approach

Eq. (41) is the generalization of the mesoscopic Young-Dupr e law (20) for the treated case with surfactant. As the concentrations are different on the wedge ($\Gamma = \Gamma_w$) and on the adsorption layer ($\Gamma = \Gamma_a$), the liquid-gas interface tensions are also different. Eq. (41) is accompanied by Eqs. (39) and (40) that provide the adsorption layer height and the relation between Γ_w and Γ_a , respectively. Comparison of the mesoscopic Young-Dupr e law [Eq. (41)] with the macroscopic one [Eq. (34) in section III A] implies

$$f(h_a, \Gamma_a) - \Gamma_a \partial_\Gamma f|_{(h_a, \Gamma_a)} = \Upsilon_{sg}(\Gamma_a) - \Upsilon_{sl} - \Upsilon(\Gamma_a) = S(\Gamma_a). \quad (42)$$

This corresponds to a generalization of the consistency condition (21) for the case with surfactant. It relates the macroscopic equations of state (or interface energies) with the height- and surfactant-dependent wetting energy.³

We have used that the surfactant concentrations should be identical in the macroscopic and the mesoscopic description. Note that the surfactant concentration Γ_w on the wedge in the mesoscopic picture corresponds to the concentration Γ_d on the droplet in the macroscopic picture, as can be seen from Eq. (37). The consistency of the surfactant concentrations in both descriptions implies another condition, namely, that the macroscopic chemical equilibrium [Eq. (24)] $\partial_\Gamma g|_{\Gamma_w} = \partial_\Gamma g_{sg}|_{\Gamma_a}$ has to coincide with the mesoscopic one [Eq. (40)], i.e., $\partial_\Gamma g|_{\Gamma_w} = \partial_\Gamma f|_{(h_a, \Gamma_a)} + \partial_\Gamma g|_{\Gamma_a}$. Comparing the two conditions implies

$$\partial_\Gamma g_{sg}|_{\Gamma_a} = \partial_\Gamma f|_{(h_a, \Gamma_a)} + \partial_\Gamma g|_{\Gamma_a}. \quad (43)$$

Introducing the resulting relation for $\partial_\Gamma f|_{(h_a, \Gamma_a)}$ into (42) results in

$$f(h_a, \Gamma_a) = g_{sg}(\Gamma_a) - \Upsilon_{sl} - g(\Gamma_a). \quad (44)$$

³ Note that alternatively one may instead of (28) define $\Upsilon = g - \Gamma \partial_\Gamma g - \Gamma/\xi \partial_\Gamma f$ rendering relations (14), (20), etc. formally valid at the cost of introducing a surfactant-, film height- and film slope-dependent surface tension.

In the next section we explore the consequences of the consistency conditions for a relatively simple case: First, we assume a low surfactant concentration resulting in purely entropic interfacial energies $g(\Gamma)$ and $g_{\text{sg}}(\Gamma)$ before extending the result to arbitrary g .

IV. APPLICATION FOR A SIMPLE ENERGY

In the next section, we illustrate our examples for a simple free energy which describes the situation of a low concentration of surfactant. We employ a wetting energy that is a product of height- and concentration-dependent factors, i.e., the presence of surfactant only changes the contact angle but not the adsorption layer height.

A. Macroscopic consideration

We consider a low concentration (ideal gas-like) insoluble surfactant on the solid-gas and the liquid-gas interface. In general, the surfactant will even in the dilute limit affect the liquid-gas and solid-gas interfaces differently, i.e., the relevant molecular scales a will differ due to different effective molecular areas. Thus we write the surface free energies $g(\Gamma)$ and $g_{\text{sg}}(\Gamma)$ as

$$g(\Gamma) = \Upsilon^0 + \frac{k_{\text{B}}T}{a^2}\Gamma(\ln \Gamma - 1) \quad (45)$$

$$g_{\text{sg}}(\Gamma) = \Upsilon_{\text{sg}}^0 + \frac{k_{\text{B}}T}{a_{\text{sg}}^2}\Gamma(\ln \Gamma - 1) \quad (46)$$

respectively, i.e., introduce different effective molecular length scales a and a_{sg} . This results in

$$\Upsilon(\Gamma) = g - \Gamma \partial_{\Gamma} g = \Upsilon^0 - \frac{k_{\text{B}}T}{a^2}\Gamma \quad (47)$$

$$\Upsilon_{\text{sg}}(\Gamma) = g_{\text{sg}} - \Gamma \partial_{\Gamma} g_{\text{sg}} = \Upsilon_{\text{sg}}^0 - \frac{k_{\text{B}}T}{a_{\text{sg}}^2}\Gamma, \quad (48)$$

i.e., the purely entropic free energy results in a linear equation of state. The macroscopic concentration-dependent $\Upsilon_{\text{sg}}(\Gamma_{\text{a}})$ reflects the fact that the solid-gas interface is 'moist' as it is covered by the adsorption layer, and at equilibrium, surfactant is found on the drop as well as on the adsorption layer. As a result, the solid-gas interface tension Υ_{sg} in the macroscopic picture aggregates the effects of surfactant on wetting energy *and* interface energy Υ .

By inserting these interface energies into the modified Young-Dupré law (34), we find

$$\cos \theta_{\text{e}} = \frac{\cos \theta_{\text{e}0} - \epsilon_1 \delta \Gamma_{\text{a}}}{1 - \epsilon_1 \Gamma_{\text{d}}} \quad (49)$$

with $\theta_{\text{e}0}$ being the contact angle in the absence of surfactant, $\delta = \frac{a^2}{a_{\text{sg}}^2}$ being the ratio of the different molecular length scales and $\epsilon_1 = k_{\text{B}}T/(a^2\Upsilon^0)$ being a positive

constant. The ratio of surfactant concentrations follows directly from Eqs. (26) as

$$\Gamma_{\text{d}} = \Gamma_{\text{a}} \frac{a^2}{a_{\text{sg}}^2} = \Gamma_{\text{a}}^{\delta}. \quad (50)$$

We discuss a number of limiting cases which distinguish between different ratios of the molecular length scales.

- (A) The dependencies of the interface energies g and g_{sg} on surfactant are identical, i.e., $a = a_{\text{sg}}$ and therefore $\delta = a^2/a_{\text{sg}}^2 = 1$. The surfactant concentrations on adsorption layer and drop are identical ($\Gamma_{\text{d}} = \Gamma_{\text{a}} = \Gamma$). The observable dependence of the equilibrium contact angle θ_{e} on the surfactant concentration takes the form

$$\cos \theta_{\text{e}} = \frac{\cos \theta_{\text{e}0} - \epsilon_1 \Gamma}{1 - \epsilon_1 \Gamma} \quad (51)$$

i.e. the contact angle would monotonically increase with the surfactant concentration, giving rise to the effect of autophobing.

- (B) The surfactant prefers to stay on the liquid-gas interface, i.e., $a \ll a_{\text{sg}}$ and $\delta = a^2/a_{\text{sg}}^2 \ll 1$. This implies $\Gamma_{\text{d}} \gg \Gamma_{\text{a}}$. The equilibrium contact angle shows the following functional dependence on the surfactant concentration

$$\cos \theta_{\text{e}} \approx \frac{\cos \theta_{\text{e}0}}{1 - \epsilon_1 \Gamma_{\text{d}}}. \quad (52)$$

This case corresponds to the classical surfactant effect, which decreases the equilibrium contact angle with increasing concentration.

- (C) The surfactant prefers to stay on the solid-gas interface, i.e., $a \gg a_{\text{sg}}$ and $\delta = a^2/a_{\text{sg}}^2 \gg 1$, which implies $\Gamma_{\text{d}} \ll \Gamma_{\text{a}}$. The equilibrium contact angle shows the following functional dependence on the surfactant concentration

$$\cos \theta_{\text{e}} \approx \cos \theta_{\text{e}0} - \epsilon_1 \delta \Gamma_{\text{d}} \quad (53)$$

This case corresponds to a strong autophobing effect, which increases the equilibrium contact angle with increasing surfactant concentration.

These limiting cases illustrate that the dependency of θ_{e} with amount of surfactant depends subtly on the nature of the free energies. This will be further investigated numerically below in section IV D.

B. Mesoscopic consideration

We again consider a low concentration (ideal gas-like) insoluble surfactant on the liquid-gas interface with the ideal gas local free energy $g(\Gamma)$ as defined in (45) and the liquid-gas interface tension $\Upsilon(\Gamma)$ as defined in (47). Note that g_{sg} does not occur in the mesoscopic description as

the whole domain is at least covered by an adsorption layer. Further we use the strong assumption that the wetting energy factorises as

$$f(h, \Gamma) = \chi(\Gamma) \hat{f}(h) \quad (54)$$

with $\chi(0) = 1$. This allows us to investigate the case of a surfactant that influences the contact angle but does not change the adsorption layer height. The surfactant-independent adsorption layer height h_a is still given by $\partial_h \hat{f}|_{h_a} = P$ as in section II B. The equilibrium contact angle θ_e is obtained by inserting the product ansatz (54) for $f(h, \Gamma)$ into (41), which results in

$$\Upsilon(\Gamma_w) \cos \theta_e = \Upsilon(\Gamma_a) + \hat{f}(h_a) [\chi(\Gamma_a) - \Gamma_a \partial_\Gamma \chi|_{\Gamma_a}]. \quad (55)$$

Note that the restriction to a simple product ansatz implies that one is not able to investigate surfactant-induced wetting transitions characterized by a diverging adsorption layer height and we expect the ansatz to break down for $\theta_e \rightarrow 0$. This will be further discussed elsewhere.⁴

C. Consistency of mesoscopic and macroscopic approach

The concentration-dependence of $\chi(\Gamma)$ in (54) can not be chosen freely, but needs to account for the consistency condition of mesoscopic and macroscopic picture (cf. sections III C). By inserting the product ansatz (54) for the wetting energy and the entropic local free energies into condition (44), which ensures the consistency of the two approaches, we obtain

$$\chi(\Gamma_a) = 1 - M \Gamma_a (\ln \Gamma_a - 1) \\ \text{with } M = \frac{k_B T}{\hat{f}(h_a)} \left(\frac{1}{a^2} - \frac{1}{a_{sg}^2} \right). \quad (56)$$

As this expression has to hold for any Γ_a , the wetting energy can be written as

$$f(h, \Gamma) = \hat{f}(h) \left[1 - \frac{k_B T}{\hat{f}(h_a)} \left(\frac{1}{a^2} - \frac{1}{a_{sg}^2} \right) \Gamma (\ln \Gamma - 1) \right]. \quad (57)$$

Let us summarize the mesoscopic and the macroscopic approach for a drop covered by insoluble surfactant: Macroscopically, the situation is completely determined

by g , g_{sg} and Υ_{sl} . This allows for given Γ_a or Γ_d to obtain the other Γ and the contact angle θ_e .

Mesoscopically, g_{sg} is not defined, but via the consistency conditions it is reflected in the wetting energy $f(h, \Gamma)$ that itself is not part of the macroscopic description. In the special case treated in this section, g is determined by a , the macroscopic quantity g_{sg} is determined by a_{sg} , and the concentration-dependence of the mesoscopic $f(h, \Gamma)$ depends on both, a and a_{sg} .

D. Numerical simulations for surfactant-covered drops on a finite domain

To illustrate the equilibrium solutions of the model for finite domains, we perform numerical time simulations of the evolution equations for film height and surfactant concentration. The emerging equilibrium states which arise in the time simulations at large times are then compared to the analytical predictions. As discussed in Refs.[13] and [14], the evolution equations for a thin film covered by an insoluble surfactant can be written in the form of a gradient dynamics of the mesoscopic free energy functional F given in Eq. (35) by introducing the projection of the surfactant concentration onto the flat surface of the substrate $\tilde{\Gamma} = \xi \Gamma$

$$\partial_t h = \nabla \cdot [Q_{hh} \nabla \frac{\delta F}{\delta h} + Q_{h\tilde{\Gamma}} \nabla \frac{\delta F}{\delta \tilde{\Gamma}}], \quad (58)$$

$$\partial_t \tilde{\Gamma} = \nabla \cdot [Q_{\tilde{\Gamma}h} \nabla \frac{\delta F}{\delta h} + Q_{\tilde{\Gamma}\tilde{\Gamma}} \nabla \frac{\delta F}{\delta \tilde{\Gamma}}], \quad (59)$$

where the respective mobilities are denoted as Q_{ij} . In the following, we consider the wetting energy

$$f(h, \Gamma) = \chi(\Gamma) \hat{f}(h) = \chi(\Gamma) \frac{A}{2h^2} \left(\frac{2h_a^3}{5h^3} - 1 \right), \quad (60)$$

where $\hat{f}(h)$ consists of two power laws and for $A > 0$ describes a partially wetting fluid that macroscopically forms a droplet of finite contact angle on a stable adsorption layer of height h_a .

For the numerical analysis, the model is re-scaled, introducing the length scale $l = h_a$. The solutions are characterized by three dimensionless parameters $\epsilon_1 = \frac{k_B T}{a^2 \Upsilon_0}$, $\epsilon_2 = -\frac{10 \hat{f}(h_a)}{3 \Upsilon_0} = \frac{A}{h_a^2 \Upsilon_0}$ and $\delta = \frac{a^2}{a_{sg}^2}$. These are connected to the ratio between the entropic contribution of the surfactant and the interfacial tension without surfactant, the equilibrium contact angle without surfactant and the ratio of the effective molecular length scales of the surfactant at the liquid-gas and solid-gas interface, respectively.

Starting with a droplet on an adsorption layer covered by a homogeneous surfactant concentration $\Gamma(x) = \bar{\Gamma}$ as initial condition, the evolution equations are solved using a finite element scheme provided by the modular toolbox DUNE-PDELAB [32, 33]. The simulation domain $\Omega = [0, L_x]$ with $L_x/l = 200$ is discretised on

⁴ In general, it is known [31] that two (independent) critical exponents characterize the change in wetting behavior close to the wetting transition: They characterize (i) how $\cos(\theta_e)$ approaches one and (ii) how the thickness of the adsorption layer diverges. Choosing a product ansatz corresponds to the limiting case of zero critical exponent for the adsorption layer height.

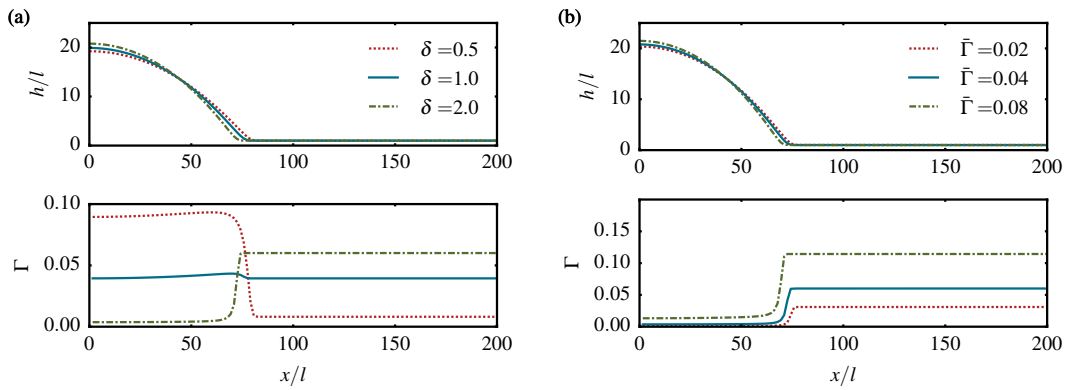


FIG. 3. Profiles of film height h (top) and surfactant concentration Γ (bottom) evolving in the numerical simulations for large times. The simulations are performed for three different ratios $\delta = \frac{a^2}{a_{sg}^2}$ of the effective molecular length scales of the surfactant at $\bar{\Gamma} = 0.04$ in (a) and three different mean surfactant concentrations $\bar{\Gamma}$ at $\delta = 2$ in (b) while keeping the remaining parameters fixed to $\epsilon_1 = 0.2$ and $\epsilon_2 = 0.4$. Note that the surfactant concentration Γ_w which occurs on the wedge in the mesoscopic description corresponds to the concentration Γ_d on the droplet.

an equidistant mesh of $N_x = 256$ quadratic elements with linear test and ansatz functions. No-flux boundary conditions are applied for both fields, corresponding to fixed amounts of fluid and surfactant in the system. For the time-integration, we employ an implicit Runge-Kutta scheme with adaptive time step and use the change in contact angle as the criterion to terminate the simulation when an equilibrium state is reached.

Figure 3 shows the profiles for film height and surfactant concentration to which the system converges for large times. As examples, we study three different ratios δ of the effective molecular length scales of the surfactant while keeping the remaining parameters fixed to $\epsilon_1 = 0.2$ and $\epsilon_2 = 0.4$. The resulting profiles confirm the limiting cases discussed in section IV A. If the dependencies of the interface energies g and g_{sg} are identical, i.e. $a = a_{sg}$ and thus $\delta = 1$ (solid blue lines), the surfactant concentration is identical on drop and adsorption layer. The addition of surfactant to the system has in this case only little effect on the contact angle. If the surfactant prefers to stay on the liquid-gas interface [$a < a_{sg}$ and thus $\delta < 1$ (dashed red lines)], the surfactant accumulates on the droplet and the contact angle is slightly lowered. If the surfactant prefers to stay on the solid-gas interface [$a > a_{sg}$ and thus $\delta > 1$ (dash-dotted green lines)], the surfactant concentration on the drop is smaller than on the adsorption layer and the contact angle of the droplet increases. From the numerical time simulations, we extract the surfactant concentrations on the adsorption layer and on the droplet as well as the equilibrium contact angle and compare it to the analytically obtained equilibrium conditions (49) and (50) using the surfactant concentration on the adsorption layer Γ_a as control parameter. In the time simulations, different amounts of surfactant are simply implemented by changing the initial concentration of surfactant $\bar{\Gamma}$. Figure 4 shows for three different values of δ the analytically ob-

tained equilibrium values (49) and (50) depending on Γ_a as solid lines and the values extracted from time simulations with $L_x/l = 200$ (diamonds). The surfactant concentrations measured in the time simulation (top) match the analytical prediction very well. However, there is a small discrepancy for the contact angles (bottom). In order to understand this offset and test the hypothesis that it can be attributed to finite size effects, we analyse the steady state solutions using parameter continuation [34] employing the software package AUTO-07p [35]. The dashed lines in Figure 4 show the concentration Γ_w and $\cos(\theta_e)$ obtained by parameter continuation for a domain and droplet size that correspond to the values used in the time simulations. If the domain size is increased to $L_x/l = 700$ with accordingly adjusted liquid volume, the values obtained by parameter continuation (dotted lines) are very close to the analytical prediction. The observed deviation of the time simulations can thus be explained by the finite size of the simulation domain and droplet. For very large domain and droplet sizes, the analytical predictions for surfactant concentration and contact angle perfectly match.

E. Generalization to arbitrary interface energies

Having established the form of the function $\chi(\Gamma)$ which guarantees the consistency of the macroscopic and mesoscopic approach for the equilibrium contact angle we can now write a free energy on the mesoscale which is consistent with the macroscale. Identifying χ with

$$\chi = \frac{1}{f_a} [g_{sg}(\Gamma) - g(\Gamma)] \quad (61)$$

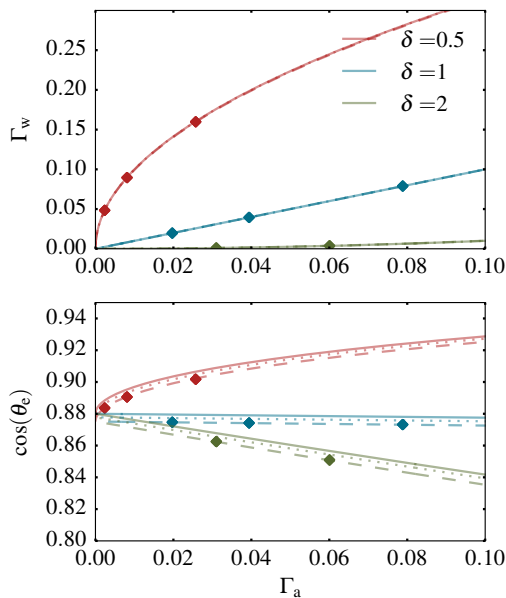


FIG. 4. Surfactant concentration on the droplet (top) and equilibrium contact angle (bottom) depending on the surfactant concentration in the adsorption layer. The analytically obtained equilibrium conditions (solid lines) are compared to values extracted from time simulations (diamonds) for three values of δ . The dashed (dotted lines) show the values obtained by parameter continuation for the domain size $L_x/l = 200$ ($L_x/l = 700$). The discrepancy in the equilibrium contact angle between the numerical and the analytical result can be attributed to finite size effects.

we can rewrite Eq. (35) as

$$F[h, \Gamma] = \int \left\{ \Upsilon_{sl} + \frac{\hat{f}(h)}{\hat{f}_a} [g_{sg}(\Gamma) - g(\Gamma)] + \xi [g(\Gamma) - \lambda\Gamma] - Ph \right\} dx. \quad (62)$$

We split now the energy functional into three contributions stemming from the droplet F_{drop} , the contact line region F_{int} and the adsorption layer F_a , i.e. $F = F_{\text{drop}} + F_{\text{int}} + F_a$. In the droplet, away from the contact line (62) simplifies to

$$F_{\text{drop}} = \int \left\{ \Upsilon_{sl} + \xi [g(\Gamma) - \lambda\Gamma] - Ph \right\} dx, \quad (63)$$

whereas in the adsorption layer we find

$$F_a = \int \left\{ \Upsilon_{sl} + g_{sg} - \lambda\Gamma \right\} dx. \quad (64)$$

where we have dropped the pressure term Ph_a in F_a by assuming that outside the adsorption layer $h \gg h_a$ and that the volume constraint on the liquid is determined by the droplet and not the adsorption layer. Expressions (63) and (64) are now identical to the macroscopic description in section III A Eq. (22). This shows that the

expression for $\chi(\Gamma)$ given in (61) is valid for all expressions g if the product ansatz for $f(h, \Gamma)$ is used.

V. CONCLUSION AND OUTLOOK

We have employed equilibrium considerations to establish the link between mesoscopic and macroscopic descriptions of drops covered by insoluble surfactants that rest on smooth solid substrates. The requirement of consistency of the two approaches relates the macroscopic quantities (interface tensions) and the mesoscopic quantities (wetting energy) and implies that the dependencies of interface and wetting energies on surfactant concentration may not be chosen independently. In particular the solid-gas interface tension in the macroscopic description is directly related to properties of the mesoscopic wetting energy.

The main conclusions of our equilibrium results also apply to the theoretical description of out-of-equilibrium phenomena through hydrodynamic modelling. In particular, the surfactant-dependencies of Derjaguin (or disjoining) pressures and interface tensions may not be chosen independently as this might result in (i) incorrect dynamics towards equilibrium and (ii) incorrect final states, i.e., that do not correspond to minima of appropriate energy functionals. We emphasize that although many phenomena associated with surfactants, like autophobing or spreading, are typically studied in dynamic and out of equilibrium settings, an underlying mesoscopic theoretical framework should for large times always lead to the same equilibrium state as the corresponding macroscopic description.

If one does not take the consistency relation into account and chooses in the mesoscopic model the surfactant-dependencies of liquid-gas interface tension and wetting energy without having the macroscopic system in mind one may implicitly assume quite peculiar surfactant-dependencies of the solid-gas interface tension.⁵

In section IV, we have used a specific simple example to illustrate how the wetting energy (and Derjaguin pressure) needs to be modified in the presence of surfactants with a linear equation of state to ensure consistency between the macroscopic and the mesoscopic picture. Note that the employed ansatz of a factorized wetting energy $f(h) = \hat{f}(h)\chi(\Gamma)$ was chosen for simplicity. It is just one possible choice and actually strongly restricts the physical phenomena that can be described. To model, e.g. the behaviour close to a wetting transition, other assumptions regarding the form of the wetting energy need to

⁵ For instance, the linear dependencies of the Hamaker and liquid-gas interface tension on surfactant concentration employed in section V.C.1 of [15] imply a solid gas interface tension of the form $c_1 + c_2\Gamma + c_3(1 + \Gamma)^{n/(m-n)}$ where the c_i are constants and n and m are the powers in a polynomial wetting energy.

be made as the product ansatz fixes the height of the adsorption layer while at a wetting transition it diverges.

The main arguments and results of our work as detailed in section III are, however, of a general nature. They are independent of the exact form of the wetting energy. We find that in the presence of surfactant, the structural form of the Young-Dupré law remains unchanged, but the surfactant concentrations and surface tensions equilibrate self-consistently. Depending on the relation of the interface free energies of liquid-gas and solid-gas interfaces, adding surfactant may have qualitatively different effects on the contact angle. Even in our simple example with purely entropic surfactant free energies, we either find a lowering of the contact angle with increasing amount of surfactant in the system or the opposite behaviour, i.e., an autophobing. The approach proposed here together with the general dynamic models introduced in [13, 14] allows for systematic numerical investigations of drop spreading and retraction dynamics employing mesoscopic models with consistent dependencies of wetting energy and interface tensions on surfactant concentration. For overviews of rich spreading, autophobing and fingering behaviour in various experiments see e.g. [3, 36–40].

As our approach is generic it may be extended to a number of more complex situations. For instance, the surfactant can accumulate at all three interfaces. Then in the macroscopic picture, the liquid-gas, solid-liquid

and solid-gas interfaces are characterized by surfactant-dependent local free energies $g(\Gamma)$, $g_{sl}(\Gamma)$, and $g_{sg}(\Gamma)$, respectively. For a fixed overall amount of surfactant one again obtains Eq. (34), however, all interface tensions correspond to local grand potentials: $\Upsilon_i = g_i(\Gamma_i) - \Gamma_i \partial_{\Gamma} g_i|_{\Gamma_i}$ and the three concentrations Γ_i are related by $\partial_{\Gamma} g|_{\Gamma=\Gamma_{lg}} = \partial_{\Gamma} g_{sl}|_{\Gamma=\Gamma_{sl}} = \partial_{\Gamma} g_{sg}|_{\Gamma=\Gamma_{sg}}$, i.e., the chemical potential is uniform across the entire system. The incorporation of surfactant also at the solid-liquid interface thus renders the discussion more involved but does not pose a principal problem as long as such a dependency is also incorporated into the mesoscale consideration. A further example is a generalization towards soluble surfactants. Then, additionally a bulk concentrations of surfactants has to be incorporated in the static consideration (for fully dynamic thin-film models see [14]). Incorporation of micelles is also possible.

In principle, the local free energies (or equation of state) for the surfactant may be arbitrarily complicated and account e.g., for phase transitions of the surfactant. This can include substrate-induced phase transitions as substrate-mediated condensation [41, 42]. If such transitions can occur the free energy also has to account for gradient contributions in the surfactant concentration (see e.g., extensions discussed in [13, 14]). The approach developed here would then again give consistency relations between interface and wetting energies and include the possibility of phase changes in the surfactant layer.

-
- [1] R. Craster and O. Matar, *Rev. Mod. Phys.* **81**, 1131 (2009).
 - [2] O. Matar and R. Craster, *Soft Matter* **5**, 3801 (2009).
 - [3] A. Marmur and M. D. Lelah, *Chem. Eng. Commun.* **13**, 133 (1981).
 - [4] S. Troian, X. Wu, and S. Safran, *Phys. Rev. Lett.* **62**, 1496 (1989).
 - [5] S. Troian, E. Herbolzheimer, and S. Safran, *Phys. Rev. Lett.* **65**, 333 (1990).
 - [6] M. Cachile, A. Cazabat, S. Bardon, M. Valignat, and F. Vandenbrouck, *Colloids Surf., A* **159**, 47 (1999).
 - [7] M. Cachile and A. Cazabat, *Langmuir* **15**, 1515 (1999).
 - [8] R. Hill, *Current opinion in colloid & interface science* **3**, 247 (1998).
 - [9] S. Rafaï, D. Sarker, V. Bergeron, J. Meunier, and D. Bonn, *Langmuir* **18**, 10486 (2002).
 - [10] A. Afsar-Siddiqui, P. Luckham, and O. Matar, *Langmuir* **20**, 7575 (2004).
 - [11] R. Craster and O. Matar, *Langmuir* **23**, 2588 (2007).
 - [12] B. Bera, M. Duits, M. Stuart, D. van den Ende, and F. Mugele, *Soft Matter* **12**, 4562 (2016).
 - [13] U. Thiele, A. J. Archer, and M. Plapp, *Phys. Fluids* **24**, 102107 (2012), note that a term was missed in the variation of F and a correction is contained in the appendix of [14].
 - [14] U. Thiele, A. J. Archer, and L. M. Pismen, *Phys. Rev. Fluids* **1**, 083903 (2016).
 - [15] M. Warner, R. Craster, and O. Matar, *Phys. Fluids* **14**, 4040 (2002).
 - [16] O. Jensen and J. Grotberg, *J. Fluid Mech.* **240**, 259 (1992).
 - [17] A. Sharma, *Langmuir* **9**, 3580 (1993).
 - [18] F. Brochard-Wyart, J.-M. di Meglio, D. QuŽerŽe, and P.-G. de Gennes, *Langmuir* **7**, 335 (1991).
 - [19] A. Oron, S. Davis, and S. Bankoff, *Rev. Mod. Phys.* **69**, 931 (1997).
 - [20] U. Thiele, *J. Phys.: Condens. Matter* **22**, 084019 (2010).
 - [21] H. Yin, D. Sibley, U. Thiele, and A. Archer, *Phys. Rev. E* **95**, 023104 (2017).
 - [22] J. H. Snoeijer and B. Andreotti, *Physics of Fluids* **20**, 057101 (2008).
 - [23] E. Bormashenko, *Colloid Surf. A-Physicochem. Eng. Asp.* **345**, 163 (2009).
 - [24] S. Dietrich (Academic Press, London, 1988) p. 1.
 - [25] M. Schick, “Introduction to wetting phenomena,” (Elsevier Science Publishers, North-Holland, 1990) p. 415.
 - [26] N. Tretyakov, M. Müller, D. Todorova, and U. Thiele, *J. Chem. Phys.* **138**, 064905 (2013).
 - [27] A. P. Hughes, U. Thiele, and A. J. Archer, *J. Chem. Phys.* **146**, 064705 (2017).
 - [28] P.-G. de Gennes, *Rev. Mod. Phys.* **57**, 827 (1985).
 - [29] L. MacDowell, *Eur. Phys. J. Special Topics* **197**, 131 (2011).
 - [30] A. P. Hughes, U. Thiele, and A. J. Archer, *J. Chem. Phys.* **142**, 074702 (2015).
 - [31] D. Bonn, J. Eggers, J. Indekeu, J. Meunier, and E. Rolley, *Rev. Mod. Phys.* **81**, 739 (2009).
 - [32] P. Bastian, M. Blatt, A. Dedner, C. Engwer, R. Klöforn,

- R. Kornhuber, M. Ohlberger, and O. Sander, *Computing* **82**, 103 (2008).
- [33] P. Bastian, M. Blatt, A. Dedner, C. Engwer, R. Klöfkorn, R. Kornhuber, M. Ohlberger, and O. Sander, *Computing* **82**, 121 (2008).
- [34] H. A. Dijkstra, F. W. Wubs, A. K. Cliffe, E. Doedel, I. F. Dragomirescu, B. Eckhardt, A. Y. Gelfgat, A. Hazel, V. Lucarini, A. G. Salinger, E. T. Phipps, J. Sanchez-Umbria, H. Schuttelaars, L. S. Tuckerman, and U. Thiele, *Commun. Comput. Phys.* **15**, 1 (2014).
- [35] E. J. Doedel and B. E. Oldeman, *AUTO07p: Continuation and Bifurcation Software for Ordinary Differential Equations*, Concordia University, Montreal (2009).
- [36] B. Frank and S. Garoff, *Langmuir* **11**, 87 (1995).
- [37] S. Bardon, M. Cachile, A. M. Cazabat, X. Fanton, M. P. Valignat, and S. Vilette, *Faraday Discuss.* , 307 (1996).
- [38] T. e. a. Stoebe, *Langmuir* **12**, 337 (1996).
- [39] V. M. Starov, S. R. Kosvintsev, and M. G. Velarde, *J. Colloid Interface Sci.* **227**, 185 (2000).
- [40] R. Sharma, R. Kalita, E. Swanson, T. Corcoran, S. Garoff, T. Przybycien, and R. Tilton, *Langmuir* **28**, 15212 (2012).
- [41] H. Riegler and K. Spratte, *Thin Solid Films* **210**, 9 (1992).
- [42] M. H. Köpf, S. V. Gurevich, R. Friedrich, and U. Thiele, *New J. Phys.* **14**, 023016 (2012).